Rheologica Acta Rheol Acta 33:473–484 (1994)

Original Contributions

Director dynamics of uniformly aligned nematic liquid crystals in transient shear flow*)

J.A. Müller, R.S. Stein, and H.H. Winter

Department of Chemical Engineering and Polymer Science and Engineering Department, University of Massachusetts, Amherst, Massachusetts, USA

Abstract: We have developed a modular rheo-optical apparatus to study the flow properties of liquid crystals. Its main components are shearing device, strong magnetic field, and optical microscope. We performed experiments on well defined initial morphologies with uniform molecular alignment. The monodomains were achieved with strong magnetic fields (4.7 T). Time-resolved conoscopy is the primary optical technique in our investigation. We propose a simple relation between the distribution of alignment angles over the sample thickness and the conoscopically measured angle, to quantitatively measure the alignment angle in shear flow.

We followed the relaxation of a shear-induced splay deformation in small molecule model systems (*N*-(*p*-methoxybenzylidene)-*p*-butylaniline (MBBA), pentyl-cyano-biphenyl (5CB) and a commercially available mixture OMI4244). We define a rotational director diffusivity $D_R = \frac{K_S}{\eta_S}$ (K_S splay elastic constant, η_S splay viscosity) from the relaxation process and devised a model, based on the diffusion equation to determine their values.

The director alignment behavior of the small molecule liquid crystals (SMLC's) in shear flow is well described by the two-dimensional Leslie-Ericksen model. The effect of director elasticity can clearly be seen in our experiments, resulting in a decrease of the steady state alignment angle at smaller Ericksen numbers.

We found that there is no strain rate dependence of the director vorticity from 0.002/s to 2/s for poly-(γ-benzyl-D/L-glutamate) (PBG). We determined $\alpha_2/\alpha_3 = -44$ for a 20% solution of 280000 molecular weight PBG in *m*-cresol at 20°C. The conoscopic interference pattern vanished after 8 strain units from an initially planar alignment and shearing could be reversed up to 10 strain units to completely recover the initial monodomain.

Key words: Liquid crystal – monodomain – conoscopy – Leslie angle – flow alignment – director diffusion

1. Introduction

A number of studies in recent years have been aimed at a better understanding of the complex balance between external fields (shear-, magnetic-, electric field) and molecular orientation of polymeric liquid crystals. Conventional rheological techniques for the characterization of the flow behavior have been complemented with optical measurements, namely small angle light scattering, polarized light microscopy, birefringence measurements, and conoscopy.

Conoscopy has been successfully used by Cladis (1972) and Pieranski and Guyon (1973, 1974) to study alignment behavior of small molecule liquid crystals. More recently Berry and Srinivasarao (1991) applied this technique to monodomains of poly(benzobisthiazole) (PBT). Liquid crystalline materials may be characterized with respect to their flow aligning behavior. They found that the material is non flow aligning in shear flow. In general, most polymeric nematogens exhibit non flow aligning behavior. How-

*) Presented at 4th Meeting of European Rheologists, Sept. 4–9, 1994, Seville, Spain

Dedicated to Prof. H. Janeschitz-Kriegl at the occasion of his 70th birthday.

ever, recently it has been shown for a semiflexible thermotropic LCP by Srinivasarao et al. (1992) that flow alignment may strongly depend on temperature. They found that the director is flow aligning when close to the nematic-isotropic transition and non flow aligning when close to the smectic-nematic transition. They interpreted their findings in terms of a sign change of one of the Leslie viscosity coefficients.

Burghardt and co-workers (1991, 1993a, b) correlated birefringence measurements with the degree of molecular orientation for textured solutions of poly(benzyl glutamate). They found a correlation between the transition zone of a low plateau and high plateau birefringence and the first normal stress difference for steady state shear.

Yang and Shine (1993) studied the stress response of uniformly aligned poly(hexyl isocyanate) and interpreted their experimental findings in the framework of the TIF (transversely isotropic fluid) model by Ericksen (1960). They were able to determine some of the Leslie viscosity coefficients.

Larson et al. (1993) recently characterized textured solutions of poly(benzyl glutamate) using polarized optical microscopy. He interpreted his experimental findings in the framework of the Ericksen number and Deborah number and observed that PBG becomes flow aligning at high Ericksen numbers, which has been predicted by molecular theory (Larson et al. 1990, 1992).

A molecular theory was first suggested by Hess (1975a, b, 1976) and has been further developed by Kuzuu and Doi (1983, 1984), Marrucci (1982, 1985) and Larson (1990) to describe the flow behavior. It is capable of predicting a region with negative first normal stress difference which has been observed earlier for solutions of poly(benzyl glutamate) by Kiss and Porter (1978, 1980).

A continuum theory for flow behavior of mesophases has been developed by Ericksen and Leslie (1960, 1962, 1966). It requires six viscosity coefficients, five of which are independent due to Parodi's (1970) relation, and three elastic constants to describe flow of a uniaxial liquid crystal. However, the theory is tailored to describe the rheological behavior of uniformly aligned nematogens, so called "monodomains", and, hence, does not account for formation and evolution of defects and texture.

This study intends to quantify the shear effects on initially uniform alignment LC fluids, and to measure the dominant material parameter. For that purpose, we built a shearing device integrated in an optical microscope and observed the effect of shear on uniformly aligned nematic liquid crystals, both small molecule and polymeric LC's. Monodomains serve as well defined initial condition for our flow experiments. Time-resolved conoscopic measurements give the tilt and twist motion of the director as a function of imposed strain and our findings are interpreted in the framework of director diffusion and the Leslie-Ericksen theory.

2. Experimental methods

2.1 Rheo-optical apparatus

Shearing device. The shearing device for simultaneous optical and rheological measurements is integrated in an optical microscope (Zeiss Universal Stand) which can be operated in conoscopic and orthoscopic mode. A schematic of the device is given in Fig. 1. The shearing unit is mounted on a base plate which is attached to the microscope stage. It can be easily detached and placed on an optical tray inside the bore of a superconducting magnet. All parts are exclusively manufactured from brass or stainless steel and allow the device to be operated in strong magnetic fields.

The lower plate is driven by an inchworm motor (Burleigh Inc.) with respect to a stationary upper plate. The linear piezo motor allows speeds in the range from below 0.1 μm/s up to 2 mm/s. Total displacement is measured by an optical encoder. A dove tail sled provides very precise and smooth motion of the moving plate.

The sample is confined between two rectangular glass slides, 25 mm × 75 mm, which are mounted in the shearing device. Spacers (Kapton sheet, glass) be-

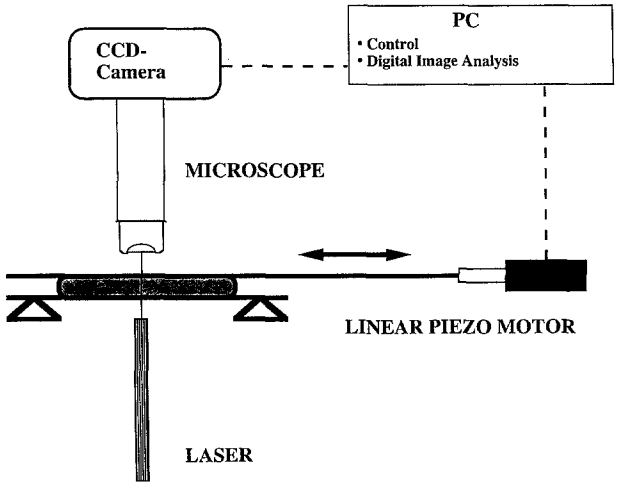

Fig. 1. Schematic of the shearing device integrated in an optical microscope

tween the glass plates, available with different thicknesses, control the distance. We used cell thicknesses between 50 μm and 750 μm.

Optical microscope. Conoscopy is the primary optical technique used in this study. It is a unique property of the conoscopic technique to distinguish between twist and tilt. Translation of the interference pattern reveals tilt of the optic axis and rotation indicates twist. Cladis (1972) demonstrated how conoscopic optics may be used to quantitatively measure twist of the optic axis. She observed the relaxation of a magnetic field induced twist deformation using conoscopy.

The sample is illuminated with monochromatic polarized light by means of a high numerical aperture condenser (0.6 – 0.75) and the highly converging light beam probes the sample simultaneously at a wide range of angles. The angle of the light cone can be as large as 75° (in air). The beam is focused in the plane of the sample and the virtual image appears in the back focal surface of the objective. Phase retardation between the ordinary and extraordinary rays results in the conoscopic interference pattern which can be related to the direction of the optic axis in a uniaxial crystal. Directions in the crystal are projected onto corresponding points in the conoscopic image. Insertion of a Amici-Bertrand lens in the microscope tube transforms the real image into the conoscopic image. This makes visible the virtual image appearing in the back focal plane of the objective. Details of the formation of conoscopic images can be found in textbooks (Wahlstrøm, 1960). A schematic in Fig. 2 shows how the conoscopic image is formed. It is advantageous in conoscopy that the material is probed simultaneously at a wide range of angles. This allows one to determine the direction of the uniaxial indicatrix, which is not possible with a beam having a single direction.

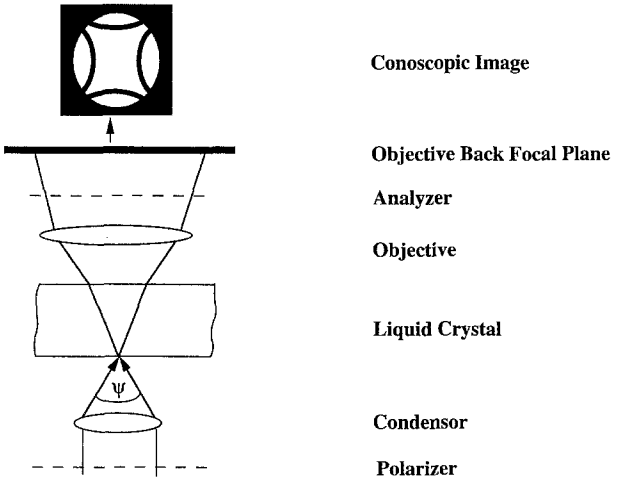

Fig. 2. Basic elements necessary for formation of a conoscopic image

The interference figure for a homeotropically and a planar aligned nematic liquid crystal are depicted in Fig. 3. The angle of the optic axis is 90° and 0°, respectively. Tilt and twist motion of the optic axis can be seen as rotation and translation of the interference pattern. The relation between the tilt angle and the translation is given by:

$$\frac{r}{R} NA = n \sin(\theta) \tag{1}$$

(r is the off center distance, R is the radius of the conoscopic image, NA the numerical aperture and n is an average refractive index of the sample, θ is the tilt angle). Equation (1) is valid for a homogeneous tilt angle and may be approximated with

$$\bar{\theta} = \frac{1}{l} \int_0^l \theta(t,y)\, dy \tag{2}$$

for a sample with distributed director angle. We use this equation for the analysis of the splay relaxation as described later. Equation (2) is considered valid for small deviations from uniform alignment.

The microscope stage micrometer allows to adjust the distance between specimen and objective. Interference patterns are recorded with a CCD camera and stored in a personal computer for subsequent image processing. The position of the fringe maxima has to be determined in order to accurately measure the amount of translation of the symmetry center. We utilize methods of digital image analysis (DIA) for this task.

2.2 Materials

Our studies have been focused on rodlike liquid crystals, solutions of poly (γ-benzylglutamate) (PBG) in *m*-cresol and small molecule liquid crystals (SMLC), namely *N*-(*p*-methoxybenzylidene)-*p*-butylaniline (MBBA), pentyl-cyano-biphenyl (5CB) and a commercially available mixture, OMI4244. The SMLC's serve as model rigid rod systems and for comparison with lyotropic PBG.

PBG is a synthetic polypeptide and very well characterized (Block, 1983). We prepared racemic mixtures of PBG with molecular weight (M_W) of 298000

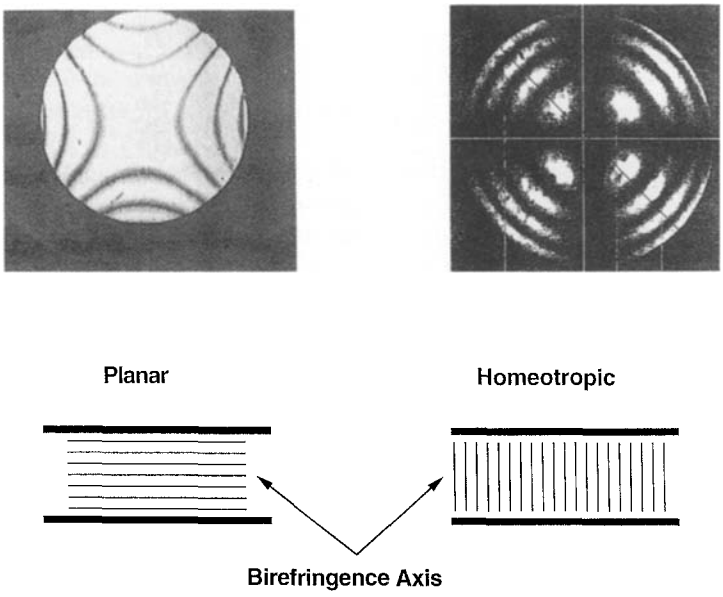

Fig. 3. Conoscopic interference pattern for planar and homeotropic alignment

(*D*-form) and 259000 (*L*-form). PBG dissolved in *m*-cresol conforms in an α-helix which is stabilized by linear hydrogen bonding and optimization of substituent packing. The chemical structure is given by:

$$-[-HNCHRCO-]_{-n} ,$$

with $R = CH_2CH_2CO_2C_6H$.

Axial ratios and rotary diffusion coefficients have been estimated by several researchers (Yang, 1958, 1959; Byerley, 1968). They concluded that PBLG remains rigid over all achievable shear rates. The existence of a well defined order in the solution state is important for correlating experimental results with theoretically predicted macromolecular behavior.

We prepared two solutions with 13% and 20% (by weight) of polymer. Solutions were stirred for 72 h and examined optically. Both solutions appeared homogeneously liquid crystalline, however, the 13% solution showed a tendency to phase separate after a few days at room temperature without stirring. This could not be observed for the 20% solution, which was stable over many days.

Other inflexible macromolecules have been studied in the past. Among those are poly(isocyanates). Aharoni (1979) and co-workers carried out intensive studies on the characterization of poly(isocyanates) in solution. However, structural conformations are less well defined as compared to poly(α-amino acids) such as PBG.

Table 1. Materials and suppliers

	MBBA	5CB	OMI4244	PBG
Supplied by	Aldrich	BDH (England)	Roche	SIGMA

2.3 Formation of uniform alignment

Surface alignment. The samples we studied were aligned uniformly. We obtained spontaneous planar alignment for the small molecule liquid crystals by coating the surfaces, which confine the sample, with a thin layer of poly vinyl alcohol and subsequent buffing. Samples were examined with polarized optical microscopy and conoscopy. The alignment was always along the buffing direction, independent of the cell filling procedure, and it was found to be indefinitely stable. Strong anchoring is critical for stable alignment.

For PBG we used a strong magnetic field to achieve uniform alignment. PBG monodomains have been prepared by Taratuta et al. (1985) and later by Hongladarom et al. (1993). A layer of silicon monoxide is vapor deposited at an oblique angle on a glass substrate. Subsequent plasma polymerization of ethylene produces a thin film of polyethylene. The resulting surface topology shows regular grooving along one axis.

For our experiments we use a simpler procedure. Before inserting the lyotropic poly(benzylglutamate), the surfaces are coated with a thin (< 100 nm) and transparent polyimide film. The film was cured at

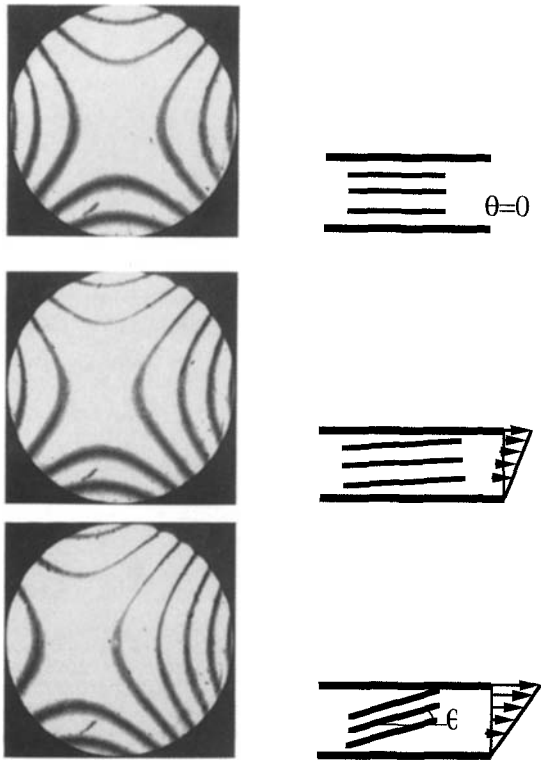

Fig. 4. Conoscopic interference pattern for different alignment angles. Pattern is shifted when optic axis is tilted

280 °C to enhance its chemical and mechanical stability and buffed subsequently.

Alignment in strong magnetic fields (lyotropic PBG). Two coated and buffed glass slides separated by 750 μm thick spacers were mounted in the flow cell. The sample, confined between the two slides, covers about 4 cm^2 of area and exhibits multi domain texture. The device is then placed inside the bore of a 4.7 T superconducting magnet (Laboratory of Dr. Sam Patz, Harvard Medical School). To follow the alignment process in situ, we mounted the shearing unit on an optical tray. The tray assembly carried all necessary components to project the conoscopic image of our sample on a screen inside the magnet bore. A schematic of the experimental configuration is given in Fig. 5. A laser is mounted on the tray with its beam going horizontally along the axis of the magnet bore. A mirror underneath the shearing unit reflects the beam vertically which then passes through polarizer and converging lense. The light cone leaving the sample passes through an analyzer and is projected on the screen above the shearing unit.

The appearance of an interference pattern on the screen indicates that uniform alignment is achieved. We can change the position where the beam is probing the sample to see if the alignment is homogeneous over the sample area. Once the sample is homogeneously aligned, the flow cell can be taken out and placed on the stage of the microscope for rheo-optical testing.

3. Results and data analysis

3.1 Transient shear flow of small molecule liquid crystal (SMLC)

We studied the director response for a shear start up situation for the SMLC's listed in Table 1 and lyotropic PBG. A schematic of 2-D shear flow situation and the coordinates used is given in Fig. 6. All samples had planar orientation before starting the experiment. It has been shown previously that MBBA

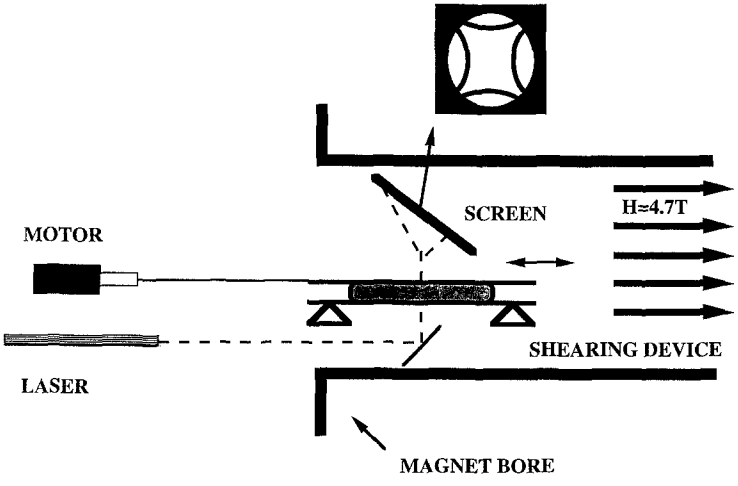

Fig. 5. Schematic of shearing device operated in strong magnetic field with in situ conoscopy. Conoscopic pattern is projected on screen inside magnet bore

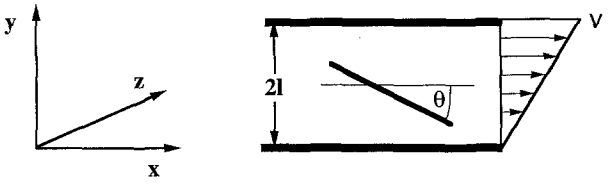

Fig. 6. Two-dimensional shear flow situation and definition of coordinates used in the analysis

and 5CB are flow aligning (Gähwiller 1971). We measured the transient director angle from initial planar alignment for a range of shear rates and Fig. 5 shows our experimental findings for MBBA. The ratio r/R, as defined in Eq. (1), is plotted on the y-axis and has been directly measured from the conoscopic images as a function of strain. For all shear rates we find that the director rotates opposite to the shear vorticity and assumes a constant value. This steady state value depends on the shear rate, being lowest for low shear rates. However, further increase in shear rate did not alter the angle once the maximum angle was reached. This angle is usually referred to as Leslie angle, θ_0, and given by

$$\tan \theta_0 = \sqrt{\frac{\alpha_3}{\alpha_2}} \,. \tag{3}$$

The Leslie angle is defined as the angle for which there is no hydrodynamic torque on the director in simple shear flow of an infinitely thick sample. A sample of finite thickness will have a gradient in director angle in y-direction. The angle is largest in the sample midplane and decreases to zero at the boundaries in case of initial planar alignment. Director angle profiles for simple shear flow situations have been calculated by Currie (1977) based upon the Leslie Ericksen equations. The profile at small Ericksen numbers can be described by a parabolic shape. However, at large Ericksen numbers the gradient will be confined in a thin boundary layer, while the bulk alignment angle is uniform.

To describe the shear start up situation we use the Leslie-Ericksen theory for two dimensions as developed by Carlsson et al. (1984, 1986). The basic equations used in our analysis are given in the appendix. The theory assumes that the director is confined in the shear plane. We could check the validity of this assumption with conoscopy. Note that the transient alignment angle is not a function of shear rate. The only parameter in this equation is the equilibrium angle, θ_0, which we have measured for our samples

Table 2. Equilibrium alignment angle for small molecule liquid crystals

Material	MBBA	OMI4244	5CB
Leslie Angle	9.2°	9.6°	22°

(see Table 2). Figure 6 shows a comparison between the experimental observations and calculations based on Eq. (A9) (see Appendix). The experimental data is well represented by the theory in the limit of high shear rates in which case the equilibrium angle is very close to the Leslie angle. However, Eq. (A9) does not describe the transient director alignment behavior at low Ericksen numbers because the terms due to director elasticity have been neglected in its derivation. Equilibrium angles lower than the Leslie angle are due to an elastic torque exerted from the sample boundaries.

Equilibrium alignment angle. Flow aligning materials may exhibit a stable angle in shear flow if it is not frustrated by instabilities. We determined the Leslie angle by slowly increasing the shear rate up to the point where the conoscopic image does not change any more over at least 20 strain units. We found the Leslie angle for MBBA to be 9.2° at 25°C. This agrees with measurements from Wahl and Fischer (1973) and Gähwiller (1971) who measured $\theta_0 = 8.2°$ and 7.1°, respectively.

However, Meiboom and Hewitt (1973) used dielectric measurement and found higher values. Figure 7

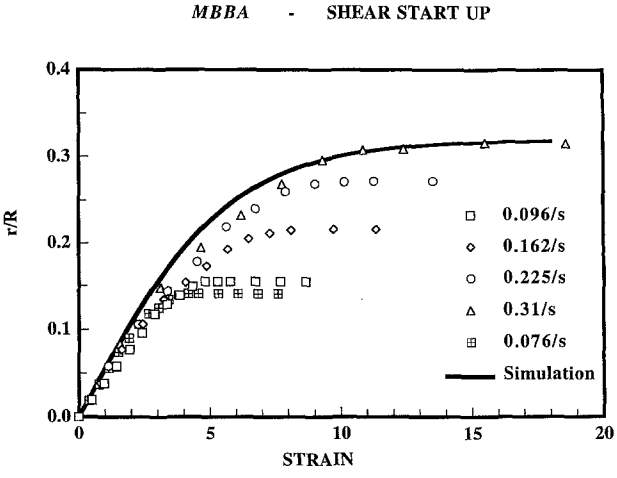

Fig. 7. Result of time-resolved conoscopic measurement for shear start up of MBBA. Sample thickness is 150 μm; 22°C

shows the angle as a function of strain at different shear rates for MBBA. Further increase of the shear rate did not alter the angle. We observed a rotation of the conoscopic image indicating a homogeneous tilt out of shear plane at higher shear rates. There has been extensive work done on the characterization of homogeneous instabilities by Dubois-Violette et al. (1977).

Splay relaxation of SMLC. The shear-induced director tilt relaxes after cessation of flow, which we observed conoscopically to determine a characteristic relaxation time. Again, boundary conditions are critical for this experiment, since the equilibrium alignment in the absence of external fields is defined by the anchoring conditions. Interestingly, we found that after filling the shear cell, uniform planar alignment is formed faster than homeotropic alignment and is also more stable to small perturbations.

For all three SMLC's, we observed an exponential decrease in the alignment angle (Fig. 8). The director profile at high Ericksen numbers for flow aligning materials can be separated in two regions, a thin boundary layer with a gradient in alignment angle and the bulk with uniform angle (Leslie angle). In the following, we suggest a phenomenological approach to analyze the relaxation process upon cessation of flow. We introduce a normalized angular displacement defined as:

$$\theta_{\mathrm{rel}} = \frac{\theta(t,y) - \theta(t=0, y=l)}{\theta_{\max} - \theta(t=0, y=l)} \,. \tag{4}$$

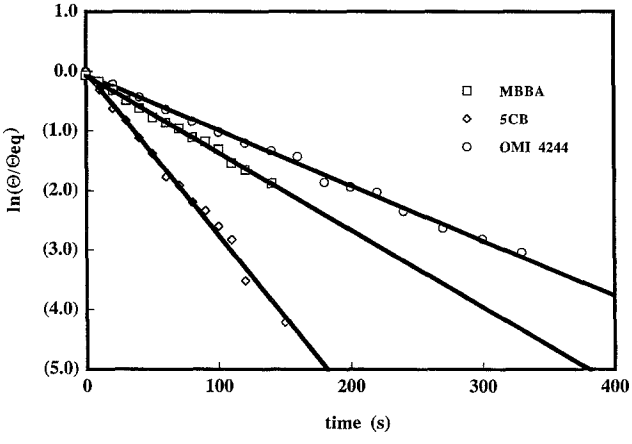

Fig. 8. Splay relaxation of three different small molecule liquid crystals. Sample thickness is 150 μm; 22 °C

For monodomains with planar alignment we take $\theta(t=0, y=l) = \theta_{\mathrm{wall}} = 0$. The quantity θ_{rel} is scaled between 0 and 1 and characterizes the state of splay relaxation with respect to the equilibrium alignment. If the director is at a maximum angular displacement from its equilibrium position, θ_{rel} will be equal to 1. However, θ_{rel} is zero in the quiescent state, when the bulk alignment is in equilibrium with its boundaries. The value of $\theta_{\max}$ will be chosen according to the initial conditions of the experiment and is given by the director angle in the sample midplane

$$\theta_{\max} = \theta(t=0, y=0) \,.$$

Our approach to analyze the flow-induced splay relaxation is motivated from a phenomenological standpoint. We assume that the evolution of the angular displacement profile over the thickness of the sample is analogous to the evolution of a concentration profile in a diffusion process, which can be described by Fick's second law:

$$\frac{\partial \theta}{\partial t} = D_R \frac{\partial^2 \theta}{\partial y^2} \,. \tag{5}$$

The diffusivity for rotation of the director in the nematic phase may be viewed as a diffusion process controlled by a quantity which we call director diffusivity. It is given by the ratio of an appropriate elastic and viscous constant, $D_R = \frac{K_S}{\eta_S}$. We will refer to D_R in the following as director diffusivity. The director profile

$$\theta(t,y) = \frac{4}{\pi} \sum_{n=0}^{\infty} \frac{(-1)^n}{2n+1} \exp\left[\frac{-D(2n+1)^2\pi^2}{4l^2} t\right] \cdot \cos\left[\frac{(2n+1)\pi y}{2l}\right] \,. \tag{6}$$

is then given as a function of time and position. In order to relate the conoscopic measurements, which give an average alignment angle over the sample thickness, we integrate Eq. (6) according to Eq. (2):

$$\bar{\theta} = \frac{8}{\pi^2} \sum_{n=0}^{\infty} \frac{1}{(2n+1)^2} \exp\left[\frac{-D_R(2n+1)^2\pi^2}{4l^2} t\right] \,. \tag{7}$$

We assume that $\bar{\theta}$ from our model calculations can be approximated with the experimentally determined angle $\overline{\theta_{CON}}$, and, hence, we can determine the director diffusion. The infinite series can be approximated by two asymptotic solutions for short times and for long times (Crank, 1956). The series can be truncated at long times for $n>0$ and we have:

$$\ln(\overline{\theta_{CON}}) = -\frac{D_R \pi^2}{4l^2} t + \text{const.} \quad \text{with } k = \frac{D_R \pi^2}{4l^2} . \tag{8}$$

Figure 8 shows the experimental results for the flow-induced splay relaxation for the small molecule liquid crystals, MBBA, 5CB and OMI4244. We calculated the corresponding alignment angle profile according to Eq. (6) at different times during the relaxation process (Fig. 9). The director diffusion, $D_R = \frac{K_S}{\eta_S}$, is calculated from the experimentally determined slope according to Eq. (8). Our results are in good agreement with previously reported values. A comparison is given in Table 3. We showed that the characteristic time constant $1/k$ increased by a factor of 4 when doubling the thickness, which follows the predicted scaling behavior.

Brochard (1972) studied the effects of secondary flow upon the relaxation from different deformations and calculated a correction factor for the characteristic relaxation time. We estimated the correction term to be smaller than 1%.

Table 3. Director diffusivities for SMLC

	MBBA	5CB	OMI4244
k (1/s)	0.0129	0.027	0.009
l (μm)	150	150	150
D_R (m²/s)	$2.9 \cdot 10^{-11}$	$6.2 \cdot 10^{-11}$	$2.1 \cdot 10^{-11}$
D_R (m²/s)	$3.5 \cdot 10^{-11}$	$7.47 \cdot 10^{-11}$	$5.7 \cdot 10^{-11}$
	Haller (1972), Gasparoux et al. (1971)	Gu et al.	(estimate from supplier)

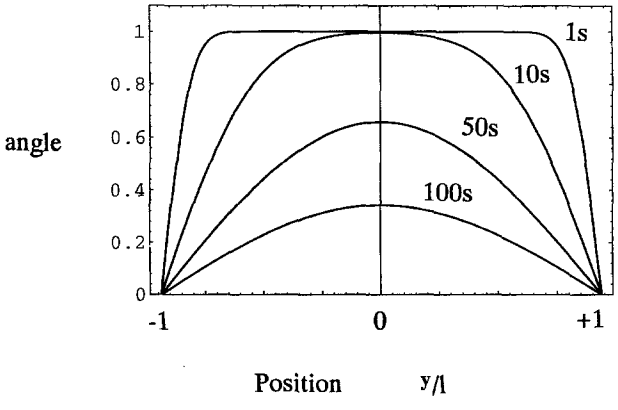

Fig. 9. Distribution of alignment angle over sample thickness during relaxation of shear-induced splay deformation

3.2 *Transient shear flow of a rodlike LCP*

We applied the same experimental techniques to lyotropic PBG as we did for the SMLC's. The monodomains were prepared and checked for their stability and alignment quality prior to the experiments by in situ conoscopy. It is important to have a uniform planar alignment of the birefringence axis throughout the sample.

The shearing unit is then placed on a specially designed microscope stage where we can record the conoscopic images. Experiments have been carried out for initially planar alignment. The sample thickness was 750 μm in all our experiments with PBG. Unfortunately, we cannot calculate an Ericksen number $\left(E_R = \frac{V2l}{D_R}, V = \text{shear velocity}, 2l = \text{sample thickness}, D_R = \frac{K_S}{\eta_S} \text{ director diffusivity}\right)$ because the values for η_S and K_S for the PBG/*m*-cresol system are unknown. However, it is possible to use the values measured by Meyer et al. (1985) for the PBG/diox-

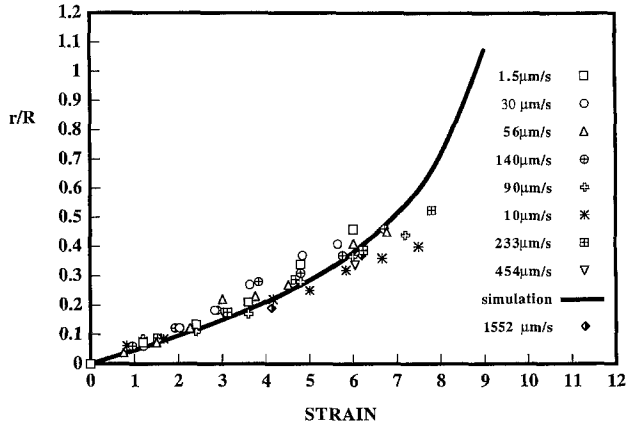

Fig. 10. Displacement of conoscopic pattern for PBG during start-up of shear flow at constant rates. Sample thickness is 750 μm; 20 °C

ane/methylenechloride system as an approximation. Figure 10 shows the displacement of the conoscopic pattern (hyperbolas for planar optic axis) plotted vs. the shear strain for shear rates from 0.002/s to 2/s. This corresponds to Ericksen numbers from about 10^3 to 10^6. The displacement is given by the dimensionless ratio r/R introduced earlier. The conoscopic pattern is lost at about 7 – 8 strain units, which indicates that the director alignment over the sampled area is inhomogeneous and there is no effective birefringence axis. Interestingly, in all our monodomain experiments (director along shearing direction) we did not see a homogeneous rotation of the director out of the shear plane with conoscopy.

In complementary orthoscopic observations we see the appearance of birefringence colors when the conoscopic pattern disappears, indicating that the director is leaving the shear plane. The birefringence colors disappear upon flow reversal, and the initial monodomain is recovered, as we saw previously with conoscopic optics.

More precisely, periodic bands perpendicular to the flow direction appear as an intermediate structure at about 7 strain units but very quickly disintegrate to form a chaotic texture at about 9 strain units. This agrees well with observations made by Srinivasarao and Berry (1991) on solutions of PBT.

The experimental data shows no strain rate dependence of the alignment dynamics over three orders of magnitude, which is in agreement with predictions by the Ericksen TIF model (Eq. (A9), Appendix). The α_2/α_3 ratio is the governing parameter in this equation and can be determined from our data. Experimentally we find α_2/α_3 to be -44 ± 5. Figure 11 shows the effect of different values of α_2/α_3 on the transient director anlge as calculated from Eq. (6b). Interestingly, the rate of rotation (director vorticity) for $\alpha_2/\alpha_3 = -1$ does not depend on the alignment angle. The director vorticity in homeotropic alignment will become much larger than the director vorticity in planar alignment for $|\alpha_2/\alpha_3| \gg 1$. The minimum vorticity occurs when the director has planar alignment and the maximum vorticity will occur for homeotropic alignment. This means that an initially slightly inhomogeneous planar alignment will either lead to premature or delayed tumbling. Hence, the onset of tumbling will randomize with increasing strain.

4. Conclusions

Conoscopy is a powerful tool for investigating the director dynamics in LC's and can be used to determine important material parameters. We found that a shear-induced splay deformation relaxes with an exponential time decay which is a measure of the director diffusion, D_R, as a characteristic material parameter. The splay relaxation process can be analyzed with the diffusion equation and director diffusivities can be determined from the slope of the decay. An analogous experiment for polymeric LC's would take place on a time scale of hours due to their much longer orientational relaxation. For flow aligning SMLC's we found that the average steady state alignment angle is a function of shear rate and approaches a limiting value, the Leslie angle.

We found PBG solutions in *m*-cresol behave non-flow aligning, known from the work of Burghardt and Fuller (1991). The rotation of the director follows the hydrodynamic vorticity and there is no stable

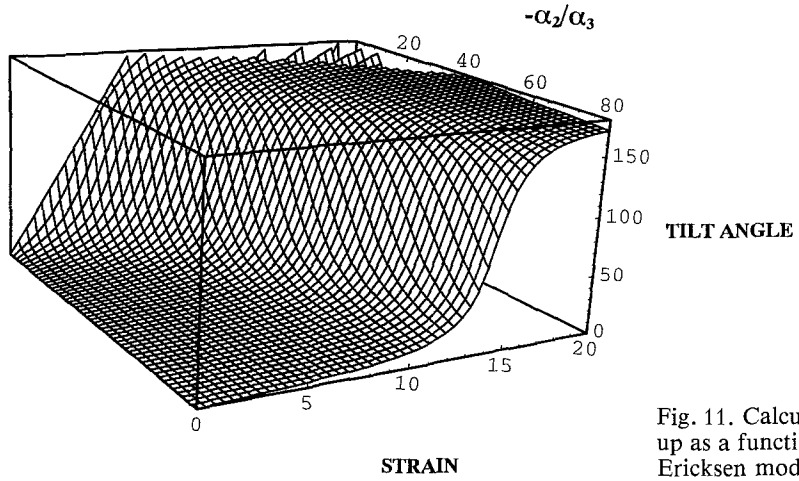

Fig. 11. Calculated director alignment angle for shear start up as a function of α_2/α_3 based on two-dimensional Leslie-Ericksen model (see Appendix)

alignment angle. The director tilt angle for shear start up was found to increase proportionally with strain but is independent of the shear rate (experiments with $\dot{\gamma}$ between 0.002/s and 2/s).

The conoscopic image vanishes at a critical shear strain of about 7 – 8, indicating that the alignment has become inhomogeneous. Conoscopy shows that there is no out-of-plane motion of the nematic director as long as the conoscopic image is still there. However, orthoscopic observations under crossed polaroids indicate that the nematic director is leaving the shear plane when the conoscopic pattern disappears. The initial monodomain can be recovered upon reversing the shear direction. The loss of the interference pattern seems also to coincide with a sudden increase in the rate of rotation of the director as predicted by the Leslie-Ericksen theory. Our observations indicate that tumbling might not be cooperative throughout the sample, instead, delayed or premature tumbling might lead to destruction of the monodomain. Interestingly, initial uniform alignment is recovered when reversing the shear direction below a total strain of 10. Rotational diffusivities, D_R, of PBG solutions are small and relaxation of the shear induced splay deformation does not occur on the time scale of our shear experiments.

Appendix

The equation for the viscous shear stress reads as follows:

$$\tau = g(\theta)\frac{\partial v}{\partial y} + (\alpha_2 \cos^2\theta - \alpha_3 \sin^2\theta)\frac{\partial \theta}{\partial t} , \qquad (A1)$$

where the viscous function $g(\theta)$ is given by

$$g(\theta) = \alpha_1 \sin^2\theta \cos^2\theta + \eta_c + (\alpha_2 + \alpha_3)\sin^2\theta . \qquad (A2)$$

The director torque balance reads as:

$$(\alpha_3 - \alpha_2)\frac{\partial \theta}{\partial t} = (\alpha_3 \sin^2\theta - \alpha_2 \cos^2\theta)\frac{\partial v}{\partial y} + h(\theta)\frac{\partial^2 \theta}{\partial y^2} + \frac{1}{2}h'(\theta)\left(\frac{\partial \theta}{\partial y}\right)^2 , \qquad (A3)$$

where the elastic function is given by:

$$h(\theta) = K_1 \sin^2\theta + K_3 \cos^2\theta \quad \text{and} \quad h'(\theta) = \frac{\partial h}{\partial \theta} . \qquad (A4)$$

When neglecting elasticity for the director torque balance, the director vorticity becomes

$$\frac{\partial \theta}{\partial t} = \frac{\alpha_3 \sin^2\theta - \alpha_2 \cos^2\theta}{\alpha_3 - \alpha_2}\dot{\gamma} . \qquad (A5)$$

This equation can be rewritten as

$$\frac{\delta^2 - 1}{\delta^2 q^2 - 1} dq = t dt , \qquad (A6)$$

with $\delta = \tan\theta_0$ and $q = \tan\theta$.

Upon integration of Eq. (A5), we have for flow-aligning materials:

$$\gamma = \frac{1}{2}\frac{\alpha_2 - \alpha_3}{\alpha_2}\sqrt{\frac{\alpha_2}{\alpha_3}} \ln\left[\frac{\sqrt{\frac{\alpha_3}{\alpha_2}}\tan\theta + 1}{\sqrt{\frac{\alpha_3}{\alpha_2}}\tan\theta - 1}\right] , \qquad (A7)$$

or equivalently:

$$\gamma = \ln\left[\left(\frac{\delta q + 1}{\delta q - 1}\right)^{[1-\delta^2/2\delta]}\right] . \qquad (A8)$$

Equation (A5) can be integrated for $\alpha_2\alpha_3 < 0$,

$$\gamma = \frac{1 + \delta^2}{\delta}\arctan(\delta \tan\theta) \left(\text{with } \delta = \sqrt{-\frac{\alpha_3}{\alpha_2}}\right) \qquad (A9)$$

and describes non flow aligning materials.

Acknowledgments

We thank Prof. Sam Patz at Harvard Medical School for his cooperation when using the superconducting magnet

and Mohan Srinivasarao for many stimulating discussions. Financial support from National Science Foundation (NSF grant DMR-9101323) is gratefully acknowledged. Equipment support came from a NEDO International Grant of Japan (PI: T. Kajiyama). The anonymous review process was conducted by Ronald Larson as member of the editorial board.

References

Aharoni SM (1979) Rigid backbone polymers. 2. Polyisocyanates and their liquid-crystal behavior. Macromolecules 12:94

Aharoni SM, Walsh EK (1979) Rigid backbone polymers. 4. Solution properties of two lyotropic mesomorphic poly(isocyanates). Macromolecules 12:271

Berry GC, Srinivasarao M (1991) Rheology of nematic solutions of rodlike chains: comparison of theory and experiment. J Stat Phys 62:1041

Block H (1983) Poly(γ-benzyl-L-glutamate) and other glutamic acid containing polymers. Gordon and Breach Science Publishers, p 215

Brochard F, Pieranski P, Guyon E (1972) Dynamics of the orientation of a nematic-liquid-crystal film in a variable magnetic field. Phys Rev Lett 28:1681

Burghardt WR, Fuller GG (1991) Role of director tumbling in the rheology of polymer liquid crystal solutions. Macromolecules 24:2546

Byerley AJ, Jennings BR, Jerrard HG (1968) Conformation parameter and gradient dependency of poly-(γ-benzyl L-glutamine) by viscometry. J Chem Phys 48:5526

Carlsson T (1984) Theoretical investigations of the shear flow of nematic liquid crystals with the Leslie viscosity $\alpha_3 > 0$: hydrodynamic analogue of first order phase transition. Molecular Crystals and Liquid Crystals 104:307

Carlsson T, Skarp K (1986) Observation of the tumbling instability in torsional shear flow of a nematic liquid crystal with $\alpha_3 > 0$. Liquid Crystals 1:455

Cladis PE (1972) New method for measuring the twist elastic constant K_{22}/χ_a and the shear viscosity γ_1/χ_a for nematics. Phys Rev Lett 28:1629

Crank J (1956) The mathematics of diffusion. Oxford at the Clarendon Press, p 347

Dubois-Violette E, Guyon E, Janossy I, Pieranski P, Manneville P (1977) Theory and experiments on plane shear flow instabilities in nematics. Journal de Mecanique 16:733

Ericksen JL (1960) Anisotropic fluids. Arch Rat Mech Anal 4:231

Ericksen JL (1962) Hydrostatic theory of liquid crystals. Arch Rat Mech Anal 9:371

Gähwiller C (1971) The viscosity coefficients of a room-temperature liquid crystal. Phys Lett 36A:311

Gasparoux H, Prost J (1971) Determination directe de l'anisotropie magnetique de crystaux liquides nematique. J Physique 32:65

Gu DF, Jamieson AM, Rosenblatt C, Tomazos D, Lee M, Percec V (1991) Dynamic light scattering from a nematic monodomain containing a side-chain liquid crystal polymer in a nematic solvent. Macromolecules 24:2385

Haller I (1972) Elastic constants of the nematic liquid crystalline phase of p-methoxybenzylidene-p-n-butylaniline (MBBA). J Chem Phys 57:1400

Hess S (1975) Irreversible thermodynamics of nonequilibrium alignment phenomena in molecular liquids and liquid crystals. Z Naturforsch 30a:728

Hess S (1975) Irreversible thermodynamics of nonequilibrium alignment phenomena in molecular liquids and liquid crystals. II. Viscous flow and flow alignment in the isotropic (stable and metastable) and nematic phases. Z Naturforsch 30a:1224

Hess S (1976) Pre- and post-transitional behavior of the flow alignment and flow-induced phase transition in liquid crystals. Z Naturforsch 31a:1507

Hongladarom K, Burghardt WR (1993) Molecular alignment of polymer liquid crystals in shear flows. 2. Transient flow behavior in poly (benzyl glutamate) solutions. Macromolecules 26:785

Hongladarom K, Burghardt WR, Baek SG, Cementwala S, Magda JJ (1993) Molecular alignment of polymer liquid crystals in shear flows. 1. Spectrographic birefringence technique, steady state orientation and normal stress behavior in poly (benzyl glutamate) solutions. Macromolecules 26:772

Kiss G, Porter RS (1978) Rheology of concentrated solutions of poly (γ-benzyl glutamate). Journal of Polymer Science: Polymer Symposium 65:193

Kiss G, Porter RS (1980) Rheo-optical studies of liquid crystalline solutions of helical polypeptides. Molecular Crystals and Liquid Crystals 60:267

Kuzuu N, Doi M (1983) Constitutive equation for nematic liquid crystals under weak velocity gradient derived from a molecular kinetic equation. Journal of the Physical Society of Japan 52:3486

Kuzuu N, Doi M (1984) Constitutive equation for nematic liquid crystals under weak velocity gradient derived from a molecular kinetic equation. II. Leslie coefficients for rodlike polymers. Journal of the Physical Society of Japan 53:1031

Larson RG (1990) Arrested tumbling in shearing flows of liquid crystal polymers. Macromolecules 23:3983

Larson RG, Mead DW (1992) Development of orientation and texture during shearing of liquid crystalline polymers. Liquid Crystals 2:751

Larson RG, Mead DW (1993) The Ericksen number and Deborah number cascades in sheared polymeric nematics. Liquid Crystals 15:151

Larson RG, Mead DW, Gleeson JT (1992) Texture of a liquid crystalline polymer during shear. Proc XIth Int Congress on Rheology Elsevier Science Publisher, Brussels, Belgium, p 65

Leslie FM (1966) Some constitutive equations for anisotropic fluids. Quart. J Mech Appl Math 19:357

MacSithigh GP, Currie PK (1977) Apparent viscosity during simple shearing flow of nematic liquid crystals. J Phys D: Appl Phys 10:1471

Marrucci G (1982) Prediction of Leslie coefficients for rodlike polymer nematics. Molecular Crystals and Liquid Crystals 72:153

Marrucci G (1985) Rheology of liquid crystalline polymers. Pure & Appl Chem 57:1545

Meiboom S, Hewitt RC (1973) Measurements of rotatioral viscosity coefficients and the shear-aligment angle in nematic liquid crystals. Phys Rev Lett 30:261

Meyer RB, Lonberg F, Taratuta V, Fraden S, Lee S-D, Hurd AJ (1985) Measurements of anisotropic viscous and elastic properties of lyotropic polymer nematics. Faraday Discuss Chem Soc 79:125

Parodi O (1970) Stress tensor for a nematic liquid crystal. J Phys (Paris) 31:581
Pieranski P, Guyon E (1973) Shear-flow-induced transition in nematics. Solid State Communications 13:435
Pieranski P, Guyon E (1974) Instabilities of certain shear flows in nematic liquids. Physical Review A9:404
Srinivasarao M, Berry G (1991) Rheo-optical studies on aligned nematic solutions of a rodlike polymer. J Rheol 35:379
Srinivasarao M, Garay RO, Winter HH, Stein RS (1992) Rheo-optical properties of a thermotropic liquid crystalline polymer. Molecular Crystals and Liquid Crystals 223:29
Taratuta VG, Srajer GM, Meyer RB (1985) Parallel alignment of poly-γ-benzyl-glutamate nematic liquid crystal at a solid surface. Molecular Crystals and Liquid Crystals 116:245
Wahl J, Fischer F (1973) Elastic and viscosity constants of nematic liquid crystals from a new optical method. Mol Cryst Liq Cryst 22:359
Wahlstrom E (1960) Optical crystallography. John Wiley & Sons, Inc. New York London, p 356
Yang I-K, Shine AD (1993) Transient shear flow of a unidomain liquid crystalline polymer. Macromolecules 26:1529
Yang JT (1958) Non-Newtonian viscosity of poly(γ-benzyl-L-glutamate) solutions. J Am Chem Soc 80:1783
Yang JT (1959) Factors affecting the non-Newtonian viscosity of rigid particles. J Am Chem Soc 81:3902

(Received August 30, 1994,
in revised form October 16, 1994)

Correspondence to:

Prof. H. Henning Winter
Dept. Chemical Engineering
University of Massachusetts
Amherst MA 01003, USA